

Break the Visual Perception: Adversarial Attacks Targeting Encoded Visual Tokens of Large Vision-Language Models

Yubo Wang
University of Science and Technology
of China
State Key Laboratory of Cognitive
Intelligence
Hefei, China
wyb123@mail.ustc.edu.cn

Chaohu Liu
University of Science and Technology
of China
State Key Laboratory of Cognitive
Intelligence
Hefei, China
liuchaohu@mail.ustc.edu.cn

Yanqiu Qu
Tencent YouTu Lab
Hefei, China
yanqiuqu@tencent.com

Haoyu Cao
Tencent YouTu Lab
Hefei, China
rechyciao@tencent.com

Deqiang Jiang
Tencent YouTu Lab
Hefei, China
dqiangjiang@tencent.com

Linli Xu*
University of Science and Technology
of China
State Key Laboratory of Cognitive
Intelligence
Hefei, China
linlixu@ustc.edu.cn

Abstract

Large vision-language models (LVLMs) integrate visual information into large language models, showcasing remarkable multi-modal conversational capabilities. However, the visual modules introduces new challenges in terms of robustness for LVLMs, as attackers can craft adversarial images that are visually clean but may mislead the model to generate incorrect answers. In general, LVLMs rely on vision encoders to transform images into visual tokens, which are crucial for the language models to perceive image contents effectively. Therefore, we are curious about one question: Can LVLMs still generate correct responses when the encoded visual tokens are attacked and disrupting the visual information? To this end, we propose a non-targeted attack method referred to as **VT-Attack** (Visual Tokens Attack), which constructs adversarial examples from multiple perspectives, with the goal of comprehensively disrupting feature representations and inherent relationships as well as the semantic properties of visual tokens output by image encoders. Using only access to the image encoder in the proposed attack, the generated adversarial examples exhibit transferability across diverse LVLMs utilizing the same image encoder and generality across different tasks. Extensive experiments validate the superior attack performance of the VT-Attack over baseline methods, demonstrating its effectiveness in attacking LVLMs with image encoders, which in turn can provide guidance on the robustness of LVLMs, particularly in terms of the stability of the visual feature space.

*Corresponding author.

Permission to make digital or hard copies of all or part of this work for personal or classroom use is granted without fee provided that copies are not made or distributed for profit or commercial advantage and that copies bear this notice and the full citation on the first page. Copyrights for components of this work owned by others than the author(s) must be honored. Abstracting with credit is permitted. To copy otherwise, or republish, to post on servers or to redistribute to lists, requires prior specific permission and/or a fee. Request permissions from permissions@acm.org.

MM '24, October 28–November 1, 2024, Melbourne, VIC, Australia.

© 2024 Copyright held by the owner/author(s). Publication rights licensed to ACM.

ACM ISBN 979-8-4007-0686-8/24/10

<https://doi.org/10.1145/3664647.3680779>

CCS Concepts

• **Computing methodologies** → **Artificial intelligence**; • **Security and privacy** → *Social aspects of security and privacy*.

Keywords

Large Vision-Language Model, Adversarial Attack, Image Encoder, Visual Tokens Attack

ACM Reference Format:

Yubo Wang, Chaohu Liu, Yanqiu Qu, Haoyu Cao, Deqiang Jiang, and Linli Xu. 2024. Break the Visual Perception: Adversarial Attacks Targeting Encoded Visual Tokens of Large Vision-Language Models. In *Proceedings of the 32nd ACM International Conference on Multimedia (MM '24)*, October 28–November 1, 2024, Melbourne, VIC, Australia. ACM, New York, NY, USA, 17 pages. <https://doi.org/10.1145/3664647.3680779>

1 Introduction

Large vision-language models (LVLMs) have garnered considerable attention owing to their remarkable visual perception and language interaction capabilities [2, 43]. Compared to large language models (LLMs), LVLMs exhibit superiority in image understanding by leveraging visual models, making them highly effective for diverse multimodal tasks, such as image captioning [23, 24], visual question answering [4] and multimodal dialogue [10, 26, 48]. However, recent research [5, 31, 47] highlights their vulnerability to adversarial attacks, posing potential security concerns in practical domains such as medical image understanding [22] and document information extraction [25]. This underscores the importance of investigating the robustness of LVLMs from an attacker's perspective.

Adversarial attacks involve the deliberate manipulation of input data to induce incorrect or specific predictions. In general, adversarial attacks can be classified into targeted attacks, which aim to mislead the model into generating specific outputs, and non-targeted attacks, which lead to any incorrect or undesired outputs.

Early research of adversarial attacks on visual models was primarily conducted to explore the security and robustness of image

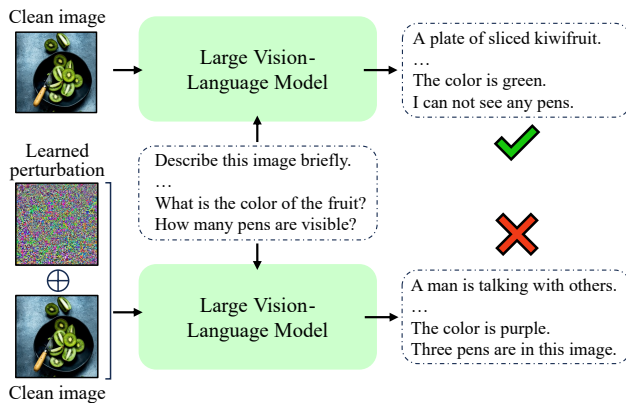


Figure 1: An example of our attack on LVLm. By adding subtle perturbation to clean image, the model fails to produce the correct answers. Even employing with various prompts, the model is unable to generate right outputs as if the visual information has become ineffective.

classification models [18, 28]. Attacking LVLms is more challenging because of a much broader prediction space, where an image can correspond to multiple textual expressions while belonging to a specific class.

Extensive investigations have been conducted to explore the robustness of LVLms, including targeted attacks [5, 31, 34, 35, 47] and non-targeted attacks [9, 34]. Specifically, the non-targeted attacks on LVLms aim to mislead models into generating any erroneous answers, which raise security concerns as these attacks can potentially lead to the breakdown of models in practical scenarios. Therefore, it is vital to design effective non-targeted attacks to investigate the robustness of multimodal systems.

Existing non-targeted attacks commonly employ end-to-end [34] or CLIP-based [9] cross-modal optimization methods, aiming to deviate images from their original textual semantics. Nevertheless, these approaches overlook the impact of manipulated visual tokens on the model robustness.

LVLms typically employ ViTs [12] as image encoders to convert images into visual tokens, which encapsulate comprehensive image features/information, working as a bridge for subsequent modules (e.g. language modules) to perceive image contents. Essentially, disrupting visual tokens can impair the model’s visual perception and ability to generate proper responses. Therefore, we suggest investigating the robustness of LVLms by conducting adversarial attacks targeting the encoded visual tokens, providing assistance for relevant research in defense.

In this paper, we propose a multi-angle attack approach called **VT-Attack** (Visual Tokens Attack) which is designed to target the image encoder of LVLms. As shown in Figure 2, our proposed approach consists of three sub-methods that systematically and comprehensively disrupt feature representations, inherent relationships, and global semantics of visual tokens output by the image encoder. This facilitates the exploration of the vulnerability of LVLms to compromised visual information in the embedding space, simulating the operations of extreme adversaries in real-world scenarios.

Notably, our approach yields two benefits. Firstly, adversarial images crafted against the shared image encoder of LVLms exhibit global effectiveness across different LVLms [35]. Secondly, we find that the adversarial perturbations obtained through the image encoders of LVLms are insensitive to specific prompts or tasks, as the generation process does not rely on the prompt/task information.

Methodologically, our method is applicable to LVLms employing ViTs [12] as image encoder. We conduct experiments on a variety of prominent baseline LVLms including LLaVA [26], MiniGPT-4 [48], LLaMA-Adapter-v2 [17], InstructBLIP [10], Otter [21], OpenFlamingo [3], BLIP-2 [24] and mPLUG-Owl-2 [42], with image encoders such as OpenAI CLIP [32], EVA CLIP [16] and other further-trained ViTs. An example of our attack is demonstrated in Figure 1. Empirical results demonstrate the effectiveness of our VT-Attack, consistently outperforming baseline approaches and individual sub-methods. Furthermore, employing adversarial examples generated against image encoders to attack downstream LVLms can successfully mislead the models into generating incorrect answers, even with different questions as prompts. We also conduct experimental analyses on the properties and functions of each sub-method to demonstrate their distinct roles in attacking from different perspectives.

In summary, our contributions can be summarized as follows:

- We propose VT-Attack, a joint method that constructs adversarial images by disrupting the visual tokens output by image encoders of LVLms from multiple perspectives, in order to investigate the robustness of LVLms against compromised visual information.
- We conduct extensive experiments on various models to demonstrate the effectiveness of the proposed method. The results indicate that the adversarial images generated by our method exhibit cross-prompt generality and enhanced attack performance over baseline methods.
- We explore the distinctive properties and contributions of each sub-method in our attack approach through experimental analysis, validating the effectiveness of the joint method.

2 Related Work

2.1 Large Vision-Language Models

Research in large vision-language models (LVLms) has been advancing rapidly, driven by the efforts of researchers who design novel model architectures and employ specific training strategies to propel their development [3, 10, 17, 21, 23, 24, 26, 42, 48].

The architecture of a large vision-language model typically comprises three components: a pre-trained image encoder, an intermediate module facilitating the transformation of visual tokens into the language space, and a large language model. Various approaches have been employed in designing the intermediate modules. For instance, LLaVA [26] utilizes linear layers to project visual features into the language space, while the BLIP-2 [24] series (MiniGPT-4 [48], InstructBLIP [10]) adopt Q-Former to extract the most relevant visual features to the text prompts for the language models.

Different LVLms may employ diverse intermediate modules for visual feature extraction, while utilizing a common pre-trained image encoder (e.g. OpenAI CLIP [32] or EVA CLIP [16]) for feature encoding. These pre-trained image encoders have been trained with

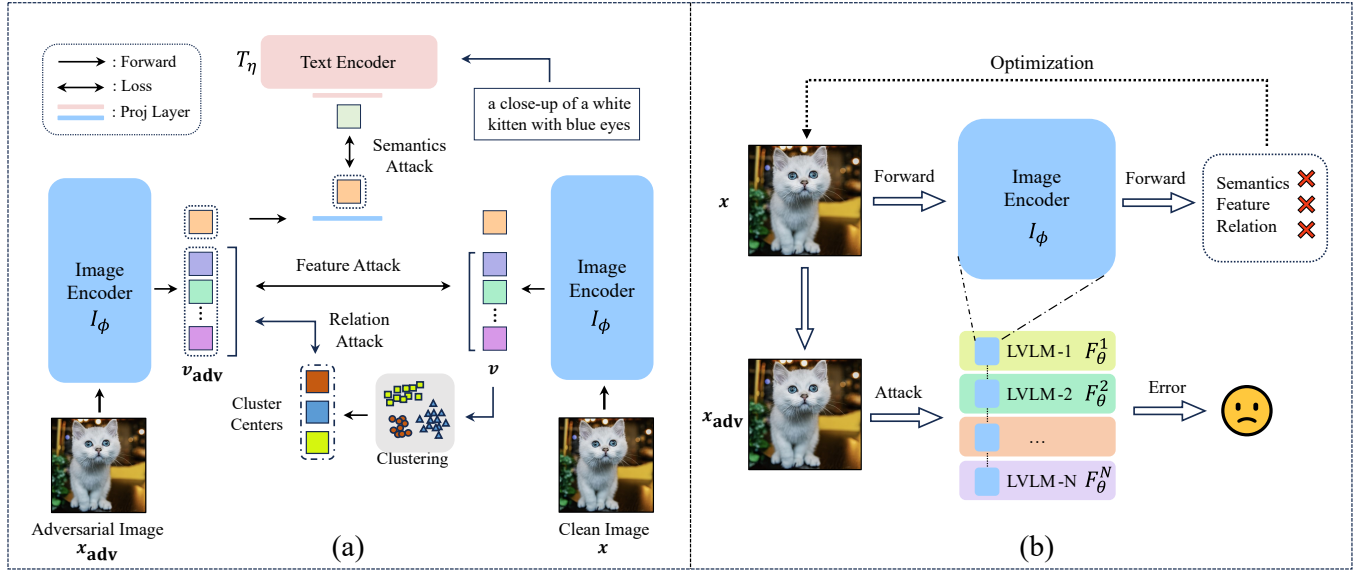


Figure 2: Unified framework for VT-Attack. (a) Both the clean image and learnable adversarial image are fed into the image encoder, yielding the [CLS] token and encoded visual tokens. The objectives of the feature attack and relation attack are to perturb visual tokens away from their original feature representations while deviating from the original cluster centers they belong to. And the aim of the semantics attack is to increase the semantic discrepancy between an image and its caption texts. (b) We first utilize the image encoder to update the adversarial perturbation, inducing the disruption of the encoded visual features at multiple levels. Next, we feed the adversarial image into various LVLMs to execute the attack.

contrastive learning on large-scale image-text datasets, allowing them to capture universal visual features that are beneficial for various downstream tasks.

2.2 Adversarial Attack

Adversarial attacks have been extensively explored to assess model robustness. Early research primarily focused on image classification, while in recent years, it has expanded into other domains [1, 36, 44, 46].

In general, adversarial attacks can be categorized into white-box attacks and black-box attacks, where white-box attacks allow attackers to have complete access to the model’s architecture and parameters [13, 28]. In contrast, black-box attacks require attackers to launch attacks without any knowledge of the model’s internal details [7, 30], making them intuitively more challenging. Because our proposed method only has access to image encoders, it can be classified into gray-box attacks, which involve partial access to the model’s architecture and parameters.

Considerable research efforts have been devoted to developing novel algorithms for adversarial attacks [6, 18, 20, 28, 37], aiming to enhance the efficiency and imperceptibility of the attacks. These studies have contributed to the gradual improvement and refinement of adversarial attack methods.

2.3 Adversarial Robustness of LVLMs

With the expanding applications of adversarial attacks, researchers have initiated investigations into the adversarial robustness of large vision-language models. LVLMs are capable of performing various

multimodal tasks, including image-text dialogue, detailed image description, and content explanation, presenting heightened challenges for adversarial attacks. Recent works have investigated the robustness of LVLMs. Among them, transferable adversarial examples are constructed using proxy models in [47], and methods such as gradient estimation are employed to attack LVLMs in black box settings. Malicious triggers are injected into the visual feature space to compromise the model security in [35]. The work in [9] conducts a comprehensive analysis on the robustness of LVLMs and devises a context-augmented image classification scheme to improve robustness. Other approaches utilize end-to-end gradient-based optimization methods to generate adversarial perturbations [5, 31, 34], typically with the cross-entropy loss as the objective to induce errors or achieve proximity between the output and a predefined target text.

Different from these works, we focus on investigating the robustness of LVLMs against impaired visual information encoded in visual tokens. We construct adversarial perturbations that disrupt visual features output by the image encoder from different perspectives, resulting in more comprehensive corruption of visual tokens and enhanced attack performance.

3 Methodology

In this section, we start with the problem formulation and then provide detailed explanations of our proposed method. The framework of our method (VT-Attack) is shown in Figure 2, where we first construct adversarial examples against image encoders and proceed to attack LVLMs.

3.1 Problem Formulation

Let $F_\theta(\mathbf{x}, \mathbf{q}) \mapsto \mathbf{z}$ denote a large visual language model parameterized by θ , where \mathbf{x} is the input image and \mathbf{q} is the prompt input to the LVLM. Let I_ϕ denote the image encoder of the LVLM parameterized by ϕ , which encodes images into visual tokens \mathbf{v} . Additionally, let M_ψ represent the intermediate module, parameterized by ψ , that processes visual tokens output by I_ϕ and transforms them into mapped visual tokens \mathbf{p} :

$$\mathbf{v} = I_\phi(\mathbf{x}), \quad \mathbf{p} = M_\psi(I_\phi(\mathbf{x}))$$

Given the input prompt \mathbf{q} and the image \mathbf{x} , the answer \mathbf{z} generated by LVLM can be represented as

$$\mathbf{z} = F_\theta(M_\psi(I_\phi(\mathbf{x})), \mathbf{q})$$

Let $\mathbf{x}_{\text{adv}} = \mathbf{x} + \Delta_{\text{adv}}$ denote the adversarial image being constructed, exhibiting subtle differences Δ_{adv} from the clean image \mathbf{x} . Our focus is on non-targeted attacks, where the adversarial image \mathbf{x}_{adv} leads the LVLM to generate any incorrect or unreasonable answers $\hat{\mathbf{y}}$ different from the original answer \mathbf{z} as follows.

$$\mathbf{z} \neq \hat{\mathbf{z}} = F_\theta(M_\psi(I_\phi(\mathbf{x} + \Delta_{\text{adv}})), \mathbf{q})$$

With only access to the parameters and gradients of the image encoder I_ϕ , our method constructs adversarial images by setting optimization objectives based on the visual tokens \mathbf{v} . During the generation process of \mathbf{x}_{adv} , it is common to apply an L_p norm constraint on the perturbation size, written as $\|\mathbf{x} - \mathbf{x}_{\text{adv}}\|_p = \|\Delta_{\text{adv}}\|_p \leq \epsilon$. It should be noted that setting ϵ to a large value may compromise the stealthiness of the generated adversarial images.

3.2 Visual Feature Representation Attack

Large vision-language models commonly employ CLIP [32] as their image encoders which are typically based on the ViT architecture [12]. An input image is split into fixed-length patches, with each patch treated as a token and fed into the ViT.

Subsequently, the ViT encodes the image and generates a series of visual tokens \mathbf{v} arranged in an $L \times D$ matrix, which can be regarded as the visual feature representation of the image. After further integration of these visual tokens by the intermediate module, the language model can naturally generate outputs leveraging the visual information.

Hence, the features output by the image encoder provides crucial visual information to the entire model. Intuitively, if the visual features are disrupted and deviated from the original representation, subsequent modules will be unable to accurately interpret the image contents, leading to erroneous model outputs.

Motivated by this, we apply a visual feature representation attack as illustrated in Figure 2 (a), aiming to maximize the loss between the feature representation in visual tokens of the adversarial image and the original representation:

$$\begin{aligned} \max \quad & \mathbb{E} \left[\sum_i \mathcal{L}(I_\phi(\mathbf{x}_{\text{adv}})^i, I_\phi(\mathbf{x})^i) \right] \\ \text{s.t.} \quad & \|\mathbf{x} - \mathbf{x}_{\text{adv}}\|_p \leq \epsilon \end{aligned} \quad (1)$$

where \mathcal{L} measures the difference or distance, which can be calculated using KL divergence or MSE. We employ the PGD [28] optimization algorithm to update the adversarial perturbations.

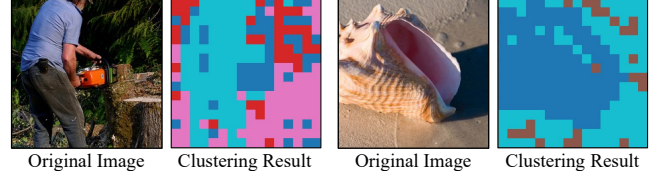


Figure 3: The comparison of original images and clustering results, where tokens/patches belonging to the same cluster are displayed in the same color.

3.3 Visual Token Relation Attack

While the visual feature attack explicitly disrupts individual visual tokens, it may not fully consider the interdependencies among these tokens. Therefore, we introduce visual token relation attack.

The self-attention [41] layers in the ViT image encoder are responsible for capturing the relationships and dependencies among image patches or tokens, corresponding to the relevance between different regions in the image [12]. These layers enable the model to weigh the importance of each token in relation to the others, allowing for a comprehensive understanding of the image's contexts.

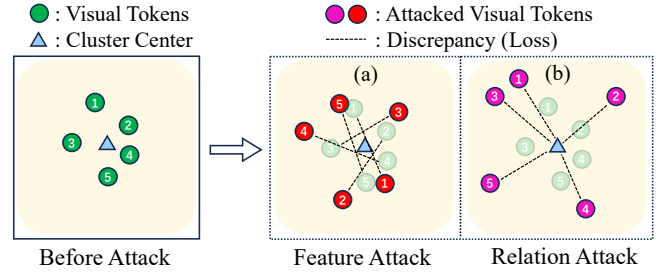


Figure 4: An illustration of feature and relation attack. (a) and (b) demonstrate potential results of attacks based on feature and attacks based on relation, respectively.

Therefore, within the visual tokens generated by the image encoder, each token tends to carry information of other tokens that have a higher degree of relationship with it. This enables the visual tokens to exhibit clustering properties, where tokens with higher correlation tend to be grouped together in the same cluster. As shown in Figure 3, visual tokens belonging to the same region or entity tend to cluster together. This clustering effect arises because tokens that are related or depict similar aspects of the image receive stronger attention connections through the self-attention mechanism.

Nevertheless, relying solely on the feature representation attack may not be sufficient to disrupt the clustering relationship among relevant visual tokens, as illustrated in Figure 4 (a). Although feature attack introduce deviations between visual tokens and their initial distribution, they may still exhibit proximity to the clustering centers.

To effectively disrupt the clustering relationships, we introduce a novel visual token relation attack, as illustrated in Figure 2 (a) and Figure 4 (b). Specifically, we initially apply the K-Means clustering [27] to the visual tokens generated by the image encoder, where the number of clusters k is determined based on the silhouette coefficient [33]. Each visual token v^i is assigned a cluster label denoted as $Y^i \in \mathcal{Y}$, and k cluster centers are identified and denoted as C :

$$\mathcal{Y} = \{Y^1, \dots, Y^L\}, C = \{C^1, \dots, C^k\} \leftarrow \text{Kmeans}(I_\phi(\mathbf{x})) \quad (2)$$

Next, we maximize the discrepancy between the visual tokens of the adversarial image and their respective cluster centers of the clean image:

$$\begin{aligned} \max \quad & \mathbb{E}[\sum_i \mathcal{L}(I_\phi(\mathbf{x}_{\text{adv}})^i, C^{Y^i})] \\ \text{s.t.} \quad & \|\mathbf{x} - \mathbf{x}_{\text{adv}}\|_p \leq \epsilon \end{aligned} \quad (3)$$

where \mathcal{L} can be measured using KL divergence or MSE. By enlarging the discrepancy between visual tokens and the original cluster centers, adversarial images can disrupt the relationships among similar visual tokens. The disruption results in reduced dependencies among tokens within each cluster, causing visual tokens to contain less local adjacent feature information. Consequently, the subsequent modules of LVLMs struggle to effectively exploit the shared information among relevant tokens to comprehend the features of neighboring image patches.

3.4 Global Semantics Attack

The feature and relation attacks introduced above directly compromise the visual token sequence of length L generated by the image encoder, resulting in disruptions at both the representation and relationship levels. While the combination of these two attacks can effectively disrupt the information of visual tokens, we are still interested in attacks that change the semantics of images.

The information carried by the [CLS] token contains the most direct content of an image, unlike the visual tokens that encode specific visual features. We hypothesize that the disruptions of both local image details (feature and relation attacks) and global semantics are mutually reinforcing, contributing to a comprehensive destruction of visual tokens.

Therefore, we incorporate the semantics attack as illustrated in Figure 2, which reduces the semantic similarity between the visual and text semantic information of the [CLS] token encoded by the CLIP image/text encoder:

$$\begin{aligned} \max \quad & \mathcal{L}(I_\phi(\mathbf{x}_{\text{adv}})^{[\text{CLS}]}, T_\eta(\mathbf{t})^{[\text{CLS}]}) \\ \text{s.t.} \quad & \|\mathbf{x} - \mathbf{x}_{\text{adv}}\|_p \leq \epsilon \end{aligned} \quad (4)$$

where T_η represents the CLIP text encoder corresponding to I_ϕ and \mathbf{t} refers to the caption of an image. We utilize cosine similarity to preserve settings similar to contrastive learning [32]. We employ a variant of cosine similarity as the loss function $\mathcal{L}(\cdot, \cdot) = \frac{1}{1 + \cos_{\text{sim}}(\cdot, \cdot)}$ to align with the loss space of the previous two methods.

Algorithm 1 VT-Attack

Require:

Image encoder I_ϕ of LVLM parameterized by ϕ , input image \mathbf{x} , image caption \mathbf{t} , CLIP text encoder T_η , perturbation size ϵ , updating rate α , optimization steps K .

Ensure:

Adversarial images \mathbf{x}_{adv} ;
1: Initialize $\mathbf{x}_{\text{adv}} = \mathbf{x} + \text{Clip}(\Delta_{\text{GaussianNoise}}, -\epsilon, \epsilon)$;
2: $\mathcal{Y} = \{Y^1, \dots, Y^L\}, C = \{C^1, \dots, C^k\} \leftarrow \text{Kmeans}(I_\phi(\mathbf{x}))$;
3: **for** $i = 1$ to K **do**
4: $\mathcal{L}_{\text{Feature}} = \mathbb{E}[\sum_i \mathcal{L}(I_\phi(\mathbf{x}_{\text{adv}})^i, I_\phi(\mathbf{x})^i)]$
5: $\mathcal{L}_{\text{Relation}} = \mathbb{E}[\sum_i \mathcal{L}(I_\phi(\mathbf{x}_{\text{adv}})^i, C^{Y^i})]$
6: $\mathcal{L}_{\text{Semantics}} = \mathcal{L}(I_\phi(\mathbf{x}_{\text{adv}})^{[\text{CLS}]}, T_\eta(\mathbf{t})^{[\text{CLS}]})$
7: $\mathcal{L} = \mathcal{L}_{\text{Feature}} + \mathcal{L}_{\text{Relation}} + \mathcal{L}_{\text{Semantics}}$
8: Gradient descent: $\mathbf{x}_{\text{adv}} = \mathbf{x}_{\text{adv}} + \alpha \cdot \text{sign}(\nabla_{\mathbf{x}_{\text{adv}}}(\mathcal{L}))$
9: Perturbation size constraint: $\mathbf{x}_{\text{adv}} = \text{Clip}_\epsilon(\mathbf{x}_{\text{adv}})$
10: Grayscale constraint: $\mathbf{x}_{\text{adv}} = \text{Clip}(\mathbf{x}_{\text{adv}}, 0, 1)$
11: **end for**
12: **return** \mathbf{x}_{adv} ;

3.5 Visual Tokens Attack (VT-Attack)

By integrating the aforementioned three sub-attack methods, we introduce a unified attack approach named VT-Attack, as illustrated in Figure 2 (a). The proposed VT-Attack can comprehensively disrupt the embedded visual features, disturb the inherent relationships and weaken the semantic properties of visual tokens, by solving the following optimization problem:

$$\begin{aligned} \max \quad & \mathcal{L}_{\text{Feature}} + \mathcal{L}_{\text{Relation}} + \mathcal{L}_{\text{Semantics}} \\ \text{s.t.} \quad & \|\mathbf{x} - \mathbf{x}_{\text{adv}}\|_p \leq \epsilon \end{aligned} \quad (5)$$

The generation process of the adversarial image is illustrated in Algorithm 1. After obtaining the adversarial image \mathbf{x}_{adv} through I_ϕ , we input it to various LVLMs that utilize I_ϕ as the image encoder, as depicted in Figure 2 (b). Due to the models' inability to perceive meaningful visual information, they tend to generate incorrect answers regardless of the types of questions concerning the image content.

4 Experiments

In this section, we present the experimental results of VT-Attack to demonstrate the effectiveness of the proposed method. Additionally, we provide experimental analysis of our approach for further exploration.

4.1 Experimental Settings

Victim models. We conduct experiments on a series of prominent baseline large vision-language models to validate the generality of our proposed method. The victim models include LLaVA [26], Otter [21], LLaMA-Adapter-v2 [17], and OpenFlamingo [3], which utilize OpenAI CLIP [32] as their image encoder, as well as BLIP-2 [24], MiniGPT-4 [48], and InstructBLIP [10], which employ EVA CLIP [16] as their image encoder. We also involve models without employing the pre-trained CLIP such as mPLUG-Owl-2 [42], utilizing a further trained ViT. We generate adversarial images using

Table 1: The results of VT-Attack on LVLMs. The evaluation metric is CLIP score(\downarrow) which measures the similarity between images and clean captions or adversarial captions generated by LVLMs. The lower the score, the higher the degree of errors in the model’s outputs, reflecting a better attack performance. "-" indicates that the attack cannot be executed due to the absence of a pre-trained text encoder. The gray background represents the attack results of the sub-methods. The best results are highlighted in bold. The best performance among the three sub-methods is highlighted in blue.

Image Encoder	OpenAI CLIP ViT				EVA CLIP ViT			ViT (Trained)
	LLaVA	Otter-I	LLaMA Adapter-v2	Open Flamingo	BLIP-2	MiniGPT-4	InstructBLIP	mPLUG Owl-2
Clean	31.94	30.87	31.49	31.95	30.44	32.45	31.07	32.61
Random Tiny Noise	31.65	30.84	31.33	31.83	30.29	32.26	31.13	32.55
E2E [34]	24.87	26.52	22.14	24.38	24.33	26.53	24.61	21.12
CLIP-Based [9]	23.24	20.04	20.19	18.53	21.56	21.72	21.47	-
Semantics	22.81	19.26	19.92	19.10	21.14	21.50	20.52	-
Feature	20.83	18.58	19.54	17.98	21.01	21.11	20.45	17.30
Relation	20.58	17.78	19.32	17.84	20.76	21.09	20.82	17.58
VT-Attack (F+R)	20.55	17.51	18.63	17.41	20.41	21.10	20.31	
VT-Attack	20.33	16.76	18.18	17.48	20.32	20.64	20.47	17.11

the ViT encoders and subsequently attack LVLMs that utilize the same image encoder.

Dataset. We follow the typical dataset construction in [11, 29, 34] by randomly sampling 1000 images from the validation set of ILSVRC 2012 for conducting adversarial attacks and evaluating robustness.

Evaluation metric. Following commonly used settings in [47], we employ the CLIP score for evaluating attack performance, which measures the similarity or alignment between images and texts. Both clean images x and adversarial images x_{adv} are fed into LVLMs to obtain clean and adversarial captions. Subsequently, we compute the CLIP scores between each image x and the clean caption z / the adversarial caption \hat{z} . The decrease in the CLIP score for the adversarial caption reflects the effectiveness of the attack. We also employ the attack success rate (ASR) used in [9]. An attack is considered successful whenever the descriptions do not align with the facts.

Basic setup. We follow the common setups in [9, 47], setting the maximum perturbation size ϵ to $8/255$ and employing the infinity norm as the constraint [47]. Note that the images are normalized. For the feature attack and relation attack, we utilize the KL divergence or MSE to compute the losses $\mathcal{L}_{Feature}$ and $\mathcal{L}_{Relation}$. The PGD algorithm [28] with 1000 iterations is employed for optimization. The learning rate is set to $1/255$. For the relation attack, we determine the optimal number of clusters k within a predefined interval using the silhouette coefficient [33].

4.2 Main Results

We conduct our evaluation primarily on the image captioning task [34, 47], as it assesses the global comprehension ability of LVLMs towards images. We query the LVLMs using the prompt "Describe the image briefly in one sentence." with adversarial images. The results are presented in Table 1. Note that "VT-Attack" refers to the combination of feature, relation and semantics attacks, while "VT-Attack (F+R)" refers to the combination of feature and relation attacks.

Table 2: The attack successful rate across different tasks (question types) by VT-Attack. Here we evaluate Otter [21] as an example. Each task is evaluated using 10 prompts (Details are provided in supplementary materials). The ASR(\uparrow) refers to the ratio of successful attacks that mislead the model’s output. The best results are highlighted in bold.

Task	Image Caption	General VQA	Detailed VQA	Avg.
Tiny Noise	0.089	0.114	0.133	0.112
E2E [34]	0.812	0.137	0.174	0.374
CLIP-Based [9]	0.851	0.289	0.635	0.592
Semantics	0.860	0.315	0.657	0.611
Feature	0.884	0.698	0.784	0.789
Relation	0.892	0.711	0.772	0.792
VT-Attack (F+R)	0.898	0.723	0.806	0.809
VT-Attack	0.914	0.715	0.828	0.816

As demonstrated in the results presented in Table 1, our proposed VT-Attack achieves the best attack performance. This indicates that our method can more extensively disrupt visual features compared to baseline methods, leading to a diminished comprehension of images by language models. Among the three sub-methods, the feature attack or relation attack typically achieves the best performance among the sub-methods, particularly the relation attack. LVLMs exhibit stronger robustness against semantics attack compared to the other two methods. However, our analysis in Section 4.3 demonstrates the insensitivity of semantics attack to image complexity.

One can also notice that, adversarial examples generated by our proposed method exhibits transferability across the LVLMs employing same image encoder, as shown in Table 1. Regardless of the intermediate modules, the LVLMs exhibit vulnerability to visual

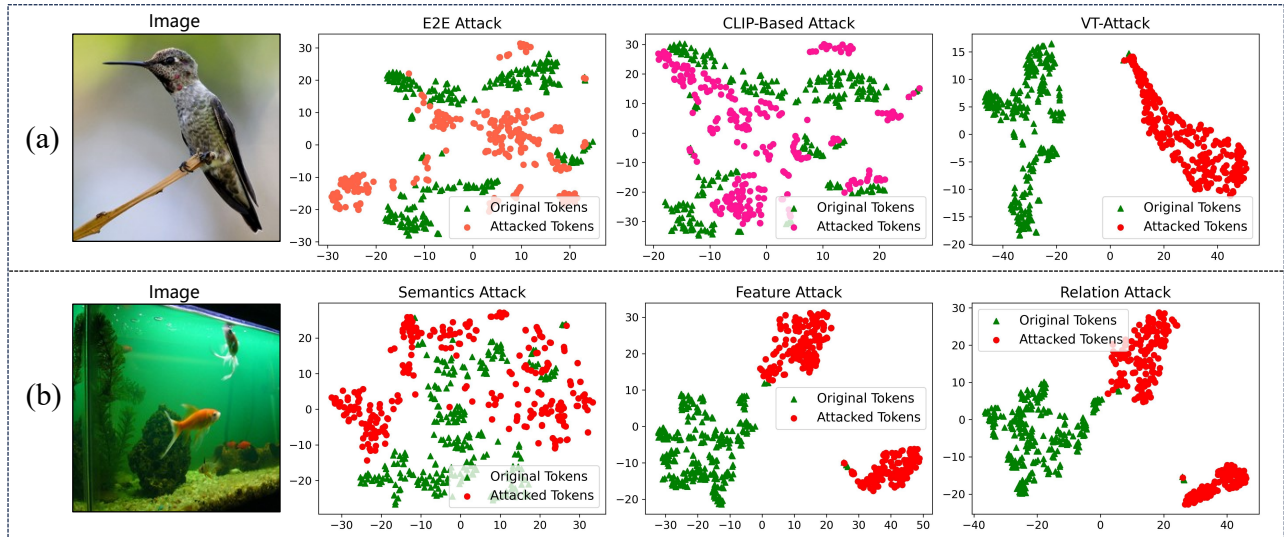


Figure 5: Original image and the reduced-dimensional distribution of attacked visual tokens. (a) Comparison of attacked visual tokens between baseline methods and VT-Attack. (b) Comparison of attacked visual tokens among the three sub-methods of VT-Attack.

tokens that lack original image information. Various intermediate modules fail to reconstruct the compromised visual content.

To further validate the generality of our method across various tasks or prompts, we conduct experiments using three different tasks, each evaluated with 10 prompts. Examples of the general VQA and the detailed VQA can be "Is there a pen in the image?" and "Please provide a detailed description of the image". More prompts are provided in supplementary materials. We employ ASR for manual evaluation and the results are shown in Table 2. Compared to baseline methods and sub-methods, VT-Attack achieves the highest ASR. We can observe that attacks against image encoders exhibit cross-task generality in contrast to end-to-end method [34]. This demonstrates the advantages of prompt-agnostic non-targeted attacks.

Table 3: Cases of attack results against LLaVA in different methods.

Image	Method	LVLm-Output
	No Attack	a dog laying on the ground
	E2E [34]	a small puppy sitting on a fence
	CLIP-Based [9]	a cat and a dog playing together
	VT-Attack	a person holding a cellphone
	No Attack	a dessert on a plate
	E2E [34]	a pastry with chocolate sauce
	CLIP-Based [9]	a plate of food with ingredients
	VT-Attack	two people are standing together

Table 3 presents cases of attacks on LLaVA [26]. Compared to the baseline methods, our attacks result in larger discrepancies between the model’s outputs and the golden captions. More cases are provided in supplementary materials. To compare the impact

of VT-Attack with baseline methods on the encoded visual tokens, we employ two-dimensional t-SNE [40] for visualization, as shown in Figure 5 (a). t-SNE is a dimensionality reduction technique that visualizes data in a lower-dimensional space, while preserving the local structure between data points. In contrast to the baseline methods, the visual tokens perturbed by VT-Attack exhibit a significant deviation from the original distribution. Such visual tokens likely have lost their original visual information, causing the language models to generate incorrect responses based on the image content.

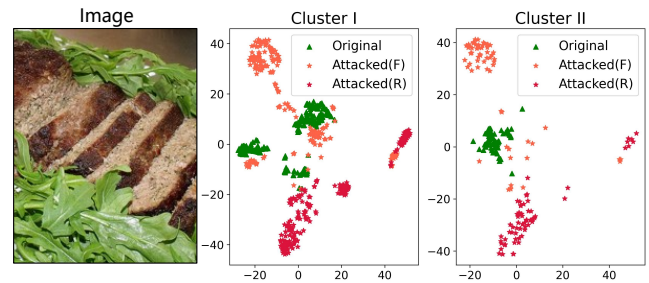


Figure 6: Visualization of the original clusters and visual tokens in the feature attack (F) and relation attack (R).

4.3 Sub-Method Analysis

Visualization of visual tokens in three different sub-methods.

In order to explore the degree of visual token disruption in each sub-method, we employ t-SNE [40] for visualization, as illustrated in Figure 5 (b). The attacked visual tokens produced by the semantics attack exhibit a distribution that remains relatively close to the original visual tokens. Nevertheless, the attacked visual tokens in the feature attack or relation attack have essentially deviated completely from the original distribution. This observation further explains why the performance of the single semantics attack is slightly lower.

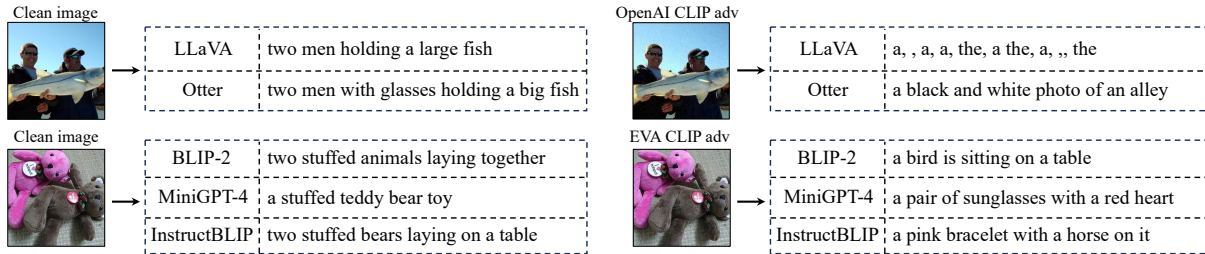


Figure 7: Comparison of the responses generated by various LVLMs when queried with clean images and adversarial images.

Comparison of visual tokens in feature and relation attack.

To identify the differences of attacked visual tokens between the feature attack and relation attack, we conduct case visualization of these two attacks in the same t-SNE space. An example is illustrated in Figure 6. We can observe that the visual tokens affected by the feature attack may still remain close to the original cluster coverage. This indicates that the incorporation of the relation attack may enhance the efficacy of disrupting the relationships between visual tokens and the original cluster, thereby compensating for the limitations of feature attack.

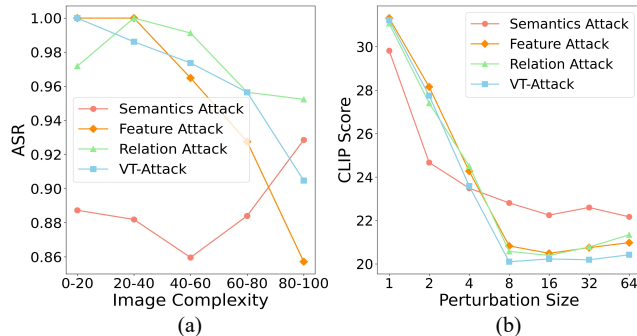


Figure 8: The influence of different conditions on attack performance against LLaVA. (a) ASR (↑) with respect to image complexity computed by segments of SAM [19]. (b) CLIP Score (↓) with respect to the perturbation size.

Semantics attack exhibit insensitivity to image complexity.

The image complexity refers to the richness exhibited by objects, colors or entities within an image. Despite the obvious impact of the feature attack and relation attack on visual tokens, their performance is influenced by the image complexity, as we have observed in our experiments. This is because the increasing image complexity amplifies the intricacy of the information in visual tokens, leading to a decreased performance. We conduct a statistical analysis of the relationship between performance (ASR) and image complexity for the three sub-methods, as illustrated in Figure 8 (a). In contrast to the other two attack, the semantics attack is not sensitive to image complexity. A possible reason is that there is no direct correlation between image semantics and complexity because an image can be described concisely even if it exhibits complexity. Therefore, the semantics attack that disrupts semantic properties is insensitive to image complexity. The results demonstrate the advantage of employing semantics attack in mitigating the limitations of feature and relation attacks.

Table 4: Perplexity of output answers for different models queried with adversarial images.

Model	LLaVA	BLIP-2	mPLUG-Owl-2
Clean	1.716	2.443	1.973
Semantics	2.165	3.261	-
Feature	4.287	2.999	2.362
Relation	4.580	3.026	2.376
VT-Attack	4.505	3.013	2.528

4.4 Further Analysis

The results of same adversarial image attacking different LVLMs. We compare the answers generated by different LVLMs given the same clean and adversarial images, as shown in Figure 7. For the same clean image, the models produce similar answers. However, the models generate completely unrelated answers for the same adversarial image. The results indicate that adversarial images lack valid visual information that can be perceived by LVLMs.

The impact of perturbation size to the performance. As shown in Figure 8 (b), the performance of the attack improves as the perturbation size increases from 1/255 to 8/255. However, further enlarging the perturbation size does not necessarily lead to performance improvement.

The impact of attacks on the perplexity of model outputs. We are curious about the self-confidence level of LVLMs in generating responses when the visual tokens are disrupted. Therefore, we compute the perplexity of the outputs from three models as shown in Table 4. The perplexity of answers corresponding to adversarial images is consistently higher than that of clean images. This indicates that the models exhibit vulnerability to compromised visual information, resulting in uncertain outputs.

5 Conclusion

In this paper, we focus on the robustness of LVLMs against non-targeted attacks. Existing methods often overlook the impact of compromised visual tokens on LVLMs. To this end, we propose a new adversarial attack method called VT-Attack, which disrupts the encoded visual tokens comprehensively from multiple perspectives. Experimental results have demonstrated the superiority of our approach over the baselines. This highlights the necessity for enhancing the adversarial defense capability of LVLMs. We hope our work can provide guidance for research on model defense, particularly in the defense of the visual token space.

Acknowledgements

This research was supported by the National Natural Science Foundation of China (Grant No. 62276245).

References

- [1] Nayyer Afaaq, Naveed Akhtar, Wei Liu, Mubarak Shah, and Ajmal Mian. 2021. Controlled Caption Generation for Images Through Adversarial Attacks. *CoRR abs/2107.03050* (2021). [arXiv:2107.03050](https://arxiv.org/abs/2107.03050) <https://arxiv.org/abs/2107.03050>
- [2] Josh Achiam, Steven Adler, Sandhini Agarwal, Lama Ahmad, Ilge Akkaya, Florencia Leoni Aleman, Diogo Almeida, Janko Altenschmidt, Sam Altman, Shyamal Anadkat, et al. 2023. Gpt-4 technical report. *arXiv preprint arXiv:2303.08774* (2023).
- [3] Anas Awadalla, Irena Gao, Josh Gardner, Jack Hessel, Yusuf Hanafy, Wamrong Zhu, Kalyani Marathe, Yonatan Bitton, Samir Gadre, Shiori Sagawa, et al. 2023. Openflamingo: An open-source framework for training large autoregressive vision-language models. *arXiv preprint arXiv:2308.01390* (2023).
- [4] Jinze Bai, Shuai Bai, Shusheng Yang, Shijie Wang, Sinan Tan, Peng Wang, Junyang Lin, Chang Zhou, and Jingren Zhou. 2023. Qwen-vl: A versatile vision-language model for understanding, localization, text reading, and beyond. (2023).
- [5] Nicholas Carlini, Milad Nasr, Christopher A. Choquette-Choo, Matthew Jagielski, Irena Gao, Pang Wei Koh, Daphne Ippolito, Florian Tramèr, and Ludwig Schmidt. 2023. Are aligned neural networks adversarially aligned?. In *Advances in Neural Information Processing Systems 36: Annual Conference on Neural Information Processing Systems 2023, NeurIPS 2023, New Orleans, LA, USA, December 10 - 16, 2023*, Alice Oh, Tristan Naumann, Amir Globerson, Kate Saenko, Moritz Hardt, and Sergey Levine (Eds.). http://papers.nips.cc/paper_files/paper/2023/hash/c1f0b856a35986348ab3414177266f75-Abstract-Conference.html
- [6] Nicholas Carlini and David A. Wagner. 2017. Towards Evaluating the Robustness of Neural Networks. In *2017 IEEE Symposium on Security and Privacy, SP 2017, San Jose, CA, USA, May 22-26, 2017*. IEEE Computer Society, 39–57. <https://doi.org/10.1109/SP.2017.49>
- [7] Pin-Yu Chen, Huan Zhang, Yash Sharma, Jinfeng Yi, and Cho-Jui Hsieh. 2017. ZOO: Zeroth Order Optimization Based Black-box Attacks to Deep Neural Networks without Training Substitute Models. In *Proceedings of the 10th ACM Workshop on Artificial Intelligence and Security, AISec@CCS 2017, Dallas, TX, USA, November 3, 2017*, Bhavani Thuraisingham, Battista Biggio, David Mandell Freeman, Brad Miller, and Arunesh Sinha (Eds.). ACM, 15–26. <https://doi.org/10.1145/3128572.3140448>
- [8] Wei-Lin Chiang, Zhuohan Li, Zi Lin, Ying Sheng, Zhanghao Wu, Hao Zhang, Lianmin Zheng, Siyuan Zhuang, Yonghao Zhuang, Joseph E. Gonzalez, Ion Stoica, and Eric P. Xing. 2023. Vicuna: An Open-Source Chatbot Impressing GPT-4 with 90%* ChatGPT Quality. <https://lmsys.org/blog/2023-03-30-vicuna/>
- [9] Xuanming Cui, Alejandro Aparcedo, Young Kyun Jang, and Ser-Nam Lim. 2023. On the Robustness of Large Multimodal Models Against Image Adversarial Attacks. *arXiv preprint arXiv:2312.03777* (2023).
- [10] Wenliang Dai, Junnan Li, Dongxu Li, Anthony Meng Huat Tiong, Junqi Zhao, Weisheng Wang, Boyang Li, Pascale Fung, and Steven C. H. Hoi. 2023. InstructBLIP: Towards General-purpose Vision-Language Models with Instruction Tuning. *CoRR abs/2305.06500* (2023). <https://doi.org/10.48550/arXiv.2305.06500>
- [11] Yinpeng Dong, Fangzhou Liao, Tianyu Pang, Hang Su, Jun Zhu, XiaoLin Hu, and Jianguo Li. 2018. Boosting adversarial attacks with momentum. In *Proceedings of the IEEE conference on computer vision and pattern recognition*. 9185–9193.
- [12] Alexey Dosovitskiy, Lucas Beyer, Alexander Kolesnikov, Dirk Weissenborn, Xiaohua Zhai, Thomas Unterthiner, Mostafa Dehghani, Matthias Minderer, Georg Heigold, Sylvain Gelly, Jakob Uszkoreit, and Neil Houlsby. 2021. An Image is Worth 16x16 Words: Transformers for Image Recognition at Scale. In *9th International Conference on Learning Representations, ICLR 2021, Virtual Event, Austria, May 3-7, 2021*. OpenReview.net. <https://openreview.net/forum?id=YicbFdNTTy>
- [13] Javid Ebrahimi, Anyi Rao, Daniel Lowd, and Dejing Dou. 2017. Hotflip: White-box adversarial examples for text classification. *arXiv preprint arXiv:1712.06751* (2017).
- [14] J Cha et al. 2024. Honeybee: Locality-enhanced Projector for Multimodal LLM.
- [15] X Dong et al. 2024. InternLM-XComposer2: Mastering Free-form Text-Image Composition and Comprehension in Vision-Language Large Model.
- [16] Yuxin Fang, Wen Wang, Binhui Xie, Quan Sun, Ledell Wu, Xinggang Wang, Tiejun Huang, Xinlong Wang, and Yue Cao. 2023. EVA: Exploring the Limits of Masked Visual Representation Learning at Scale. In *IEEE/CVF Conference on Computer Vision and Pattern Recognition, CVPR 2023, Vancouver, BC, Canada, June 17-24, 2023*. IEEE, 19358–19369. <https://doi.org/10.1109/CVPR52729.2023.01855>
- [17] Peng Gao, Jiaming Han, Renrui Zhang, Ziyi Lin, Shijie Geng, Aojun Zhou, Wei Zhang, Pan Lu, Conghui He, Xiangyu Yue, Hongsheng Li, and Yu Qiao. 2023. LLaMA-Adapter V2: Parameter-Efficient Visual Instruction Model. *CoRR abs/2304.15010* (2023). <https://doi.org/10.48550/ARXIV.2304.15010>
- [18] Ian J. Goodfellow, Jonathon Shlens, and Christian Szegedy. 2015. Explaining and Harnessing Adversarial Examples. In *3rd International Conference on Learning Representations, ICLR 2015, San Diego, CA, USA, May 7-9, 2015, Conference Track Proceedings*, Yoshua Bengio and Yann LeCun (Eds.). <http://arxiv.org/abs/1412.6572>
- [19] Alexander Kirillov, Eric Mintun, Nikhila Ravi, Hanzi Mao, Chloé Rolland, Laura Gustafson, Kete Xiao, Spencer Whitehead, Alexander C. Berg, Wan-Yen Lo, Piotr Dollár, and Ross B. Girshick. 2023. Segment Anything. In *IEEE/CVF International Conference on Computer Vision, ICCV 2023, Paris, France, October 1-6, 2023*. IEEE, 3992–4003. <https://doi.org/10.1109/ICCV51070.2023.00371>
- [20] Alexey Kurakin, Ian J. Goodfellow, and Samy Bengio. 2017. Adversarial examples in the physical world. In *5th International Conference on Learning Representations, ICLR 2017, Toulon, France, April 24-26, 2017, Workshop Track Proceedings*. OpenReview.net. <https://openreview.net/forum?id=HJGU3Rodl>
- [21] Bo Li, Yuanhan Zhang, Liangyu Chen, Jinghao Wang, Jingkang Yang, and Zhiwei Liu. 2023. Otter: A Multi-Modal Model with In-Context Instruction Tuning. *CoRR abs/2305.03726* (2023). <https://doi.org/10.48550/ARXIV.2305.03726>
- [22] Chunyuan Li, Cliff Wong, Sheng Zhang, Naoto Usuyama, Haotian Liu, Jianwei Yang, Tristan Naumann, Hoifung Poon, and Jianfeng Gao. 2024. Llava-med: Training a large language-and-vision assistant for biomedicine in one day. *Advances in Neural Information Processing Systems 36* (2024).
- [23] Chenliang Li, Haiyang Xu, Junfeng Tian, Wei Wang, Ming Yan, Bin Bi, Jiabo Ye, He Chen, Guohai Xu, Zheng Cao, Ji Zhang, Songfang Huang, Fei Huang, Jingren Zhou, and Luo Si. 2022. mPLUG: Effective and Efficient Vision-Language Learning by Cross-modal Skip-connections. In *Proceedings of the 2022 Conference on Empirical Methods in Natural Language Processing, EMNLP 2022, Abu Dhabi, United Arab Emirates, December 7-11, 2022*, Yoav Goldberg, Zornitsa Kozareva, and Yue Zhang (Eds.). Association for Computational Linguistics, 7241–7259. <https://doi.org/10.18653/V1/2022.EMNLP-MAIN.488>
- [24] Junnan Li, Dongxu Li, Silvio Savarese, and Steven C. H. Hoi. 2023. BLIP-2: Bootstrapping Language-Image Pre-training with Frozen Image Encoders and Large Language Models. In *International Conference on Machine Learning, ICML 2023, 23-29 July 2023, Honolulu, Hawaii, USA (Proceedings of Machine Learning Research, Vol. 202)*, Andreas Krause, Emma Brunskill, Kyunghyun Cho, Barbara Engelhardt, Sivan Sabato, and Jonathan Scarlett (Eds.). PMLR, 19730–19742. <https://proceedings.mlr.press/v202/li23q.html>
- [25] Chaohu Liu, Kun Yin, Haoyu Cao, Xinghua Jiang, Xin Li, Yinsong Liu, Deqiang Jiang, Xing Sun, and Linli Xu. 2024. HRVDA: High-Resolution Visual Document Assistant. *arXiv:2404.06918* [cs.CV]
- [26] Haotian Liu, Chunyuan Li, Qingyang Wu, and Yong Jae Lee. 2023. Visual Instruction Tuning. *CoRR abs/2304.08485* (2023). <https://doi.org/10.48550/arXiv.2304.08485>
- [27] Stuart P. Lloyd. 1982. Least squares quantization in PCM. *IEEE Trans. Inf. Theory* 28, 2 (1982), 129–136. <https://doi.org/10.1109/TIT.1982.1056489>
- [28] Aleksander Madry, Aleksandar Makelov, Ludwig Schmidt, Dimitris Tsipras, and Adrian Vladu. 2018. Towards Deep Learning Models Resistant to Adversarial Attacks. In *6th International Conference on Learning Representations, ICLR 2018, Vancouver, BC, Canada, April 30 - May 3, 2018, Conference Track Proceedings*. OpenReview.net. <https://openreview.net/forum?id=rjzBfZAb>
- [29] Kaleel Mahmood, Rigel Mahmood, and Marten van Dijk. 2021. On the Robustness of Vision Transformers to Adversarial Examples. In *2021 IEEE/CVF International Conference on Computer Vision, ICCV 2021, Montreal, QC, Canada, October 10-17, 2021*. IEEE, 7818–7827. <https://doi.org/10.1109/ICCV48922.2021.00774>
- [30] Nicolas Papernot, Patrick D. McDaniel, and Ian J. Goodfellow. 2016. Transferability in Machine Learning: from Phenomena to Black-Box Attacks using Adversarial Samples. *CoRR abs/1605.07277* (2016). [arXiv:1605.07277](http://arxiv.org/abs/1605.07277) <http://arxiv.org/abs/1605.07277>
- [31] Xiangyu Qi, Kaixuan Huang, Ashwinee Panda, Peter Henderson, Mengdi Wang, and Prateek Mittal. 2024. Visual Adversarial Examples Jailbreak Aligned Large Language Models. In *Thirty-Eighth AAAI Conference on Artificial Intelligence, AAAI 2024, Thirty-Sixth Conference on Innovative Applications of Artificial Intelligence, IAAI 2024, Fourteenth Symposium on Educational Advances in Artificial Intelligence, EAAI 2024, February 20-27, 2024, Vancouver, Canada*, Michael J. Wooldridge, Jennifer G. Dy, and Sriraam Natarajan (Eds.). AAAI Press, 21527–21536. <https://doi.org/10.1609/AAAI.V38I19.30150>
- [32] Alec Radford, Jong Wook Kim, Chris Hallacy, Aditya Ramesh, Gabriel Goh, Sandhini Agarwal, Girish Sastry, Amanda Askell, Pamela Mishkin, Jack Clark, Gretchen Krueger, and Ilya Sutskever. 2021. Learning Transferable Visual Models From Natural Language Supervision. In *Proceedings of the 38th International Conference on Machine Learning, ICML 2021, 18-24 July 2021, Virtual Event (Proceedings of Machine Learning Research, Vol. 139)*, Marina Meila and Tong Zhang (Eds.). PMLR, 8748–8763. <http://proceedings.mlr.press/v139/radford21a.html>
- [33] Peter J Rousseeuw. 1987. Silhouettes: a graphical aid to the interpretation and validation of cluster analysis. *Journal of computational and applied mathematics* 20 (1987), 53–65.
- [34] Christian Schlarman and Matthias Hein. 2023. On the Adversarial Robustness of Multi-Modal Foundation Models. In *IEEE/CVF International Conference on Computer Vision, ICCV 2023 - Workshops, Paris, France, October 2-6, 2023*. IEEE, 3679–3687. <https://doi.org/10.1109/ICCVW60793.2023.00395>

- [35] Erfan Shayegani, Yue Dong, and Nael Abu-Ghazaleh. 2023. Jailbreak in pieces: Compositional adversarial attacks on multi-modal language models. In *The Twelfth International Conference on Learning Representations*.
- [36] Sasha Sheng, Amanpreet Singh, Vedanuj Goswami, Jose Alberto Lopez Magana, Tristan Thrush, Wojciech Galuba, Devi Parikh, and Douwe Kiela. 2021. Human-Adversarial Visual Question Answering. In *Advances in Neural Information Processing Systems 34: Annual Conference on Neural Information Processing Systems 2021, NeurIPS 2021, December 6–14, 2021, virtual*, Marc’Aurelio Ranzato, Alina Beygelzimer, Yann N. Dauphin, Percy Liang, and Jennifer Wortman Vaughan (Eds.), 20346–20359. <https://proceedings.neurips.cc/paper/2021/hash/aa97d584861474f4097cf13ccb5325da-Abstract.html>
- [37] Christian Szegedy, Wojciech Zaremba, Ilya Sutskever, Joan Bruna, Dumitru Erhan, Ian J. Goodfellow, and Rob Fergus. 2014. Intriguing properties of neural networks. In *2nd International Conference on Learning Representations, ICLR 2014, Banff, AB, Canada, April 14–16, 2014, Conference Track Proceedings*, Yoshua Bengio and Yann LeCun (Eds.). <http://arxiv.org/abs/1312.6199>
- [38] MosaicML NLP Team. 2023. *Introducing MPT-7B: A New Standard for Open-Source, Commercially Usable LLMs*. www.mosaicml.com/blog/mpt-7b Accessed: 2023-05-05.
- [39] Hugo Touvron, Thibaut Lavril, Gautier Izacard, Xavier Martinet, Marie-Anne Lachaux, Timothée Lacroix, Baptiste Rozière, Naman Goyal, Eric Hambro, Faisal Azhar, Aurelien Rodriguez, Armand Joulin, Edouard Grave, and Guillaume Lample. 2023. LLaMA: Open and Efficient Foundation Language Models. arXiv:2302.13971 [cs.CL]
- [40] Laurens Van der Maaten and Geoffrey Hinton. 2008. Visualizing data using t-SNE. *Journal of machine learning research* 9, 11 (2008).
- [41] Ashish Vaswani, Noam Shazeer, Niki Parmar, Jakob Uszkoreit, Llion Jones, Aidan N. Gomez, Lukasz Kaiser, and Illia Polosukhin. 2017. Attention is All you Need. In *Advances in Neural Information Processing Systems 30: Annual Conference on Neural Information Processing Systems 2017, December 4–9, 2017, Long Beach, CA, USA*, Isabelle Guyon, Ulrike von Luxburg, Samy Bengio, Hanna M. Wallach, Rob Fergus, S. V. N. Vishwanathan, and Roman Garnett (Eds.), 5998–6008. <https://proceedings.neurips.cc/paper/2017/hash/3f5ee243547dee91fbd053c1c4a845aa-Abstract.html>
- [42] Qinghao Ye, Haiyang Xu, Jiabo Ye, Ming Yan, Haowei Liu, Qi Qian, Ji Zhang, Fei Huang, and Jingren Zhou. 2023. mplug-owl2: Revolutionizing multi-modal large language model with modality collaboration. *arXiv preprint arXiv:2311.04257* (2023).
- [43] Shukang Yin, Chaoyou Fu, Sirui Zhao, Ke Li, Xing Sun, Tong Xu, and Enhong Chen. 2023. A Survey on Multimodal Large Language Models. *CoRR* abs/2306.13549 (2023). <https://doi.org/10.48550/arXiv.2306.13549>
- [44] Jiaming Zhang, Qi Yi, and Jitao Sang. 2022. Towards Adversarial Attack on Vision-Language Pre-training Models. In *MM '22: The 30th ACM International Conference on Multimedia, Lisboa, Portugal, October 10 - 14, 2022*, João Magalhães, Alberto Del Bimbo, Shin’ichi Satoh, Nicu Sebe, Xavier Alameda-Pineda, Qin Jin, Vincent Oria, and Laura Toni (Eds.). ACM, 5005–5013. <https://doi.org/10.1145/3503161.3547801>
- [45] Susan Zhang, Stephen Roller, Naman Goyal, Mikel Artetxe, Moya Chen, Shuohui Chen, Christopher Dewan, Mona Diab, Xian Li, Xi Victoria Lin, Todor Mihaylov, Myle Ott, Sam Shleifer, Kurt Shuster, Daniel Simig, Punit Singh Koura, Anjali Sridhar, Tianlu Wang, and Luke Zettlemoyer. 2022. OPT: Open Pre-trained Transformer Language Models. arXiv:2205.01068 [cs.CL]
- [46] Shaofeng Zhang, Zheng Wang, Xing Xu, Xiang Guan, and Yang Yang. 2020. Fooled by Imagination: Adversarial Attack to Image Captioning Via Perturbation in Complex Domain. In *IEEE International Conference on Multimedia and Expo, ICME 2020, London, UK, July 6–10, 2020*. IEEE, 1–6. <https://doi.org/10.1109/ICME46284.2020.9102842>
- [47] Yunqing Zhao, Tianyu Pang, Chao Du, Xiao Yang, Chongxuan Li, Ngai-Man Cheung, and Min Lin. 2023. On Evaluating Adversarial Robustness of Large Vision-Language Models. In *Advances in Neural Information Processing Systems 36: Annual Conference on Neural Information Processing Systems 2023, NeurIPS 2023, New Orleans, LA, USA, December 10 - 16, 2023*, Alice Oh, Tristan Naumann, Amir Globerson, Kate Saenko, Moritz Hardt, and Sergey Levine (Eds.). http://papers.nips.cc/paper_files/paper/2023/hash/a97b58c4f7551053b0512f92244b0810-Abstract-Conference.html
- [48] Deyao Zhu, Jun Chen, Xiaoqian Shen, Xiang Li, and Mohamed Elhoseiny. 2023. MiniGPT-4: Enhancing Vision-Language Understanding with Advanced Large Language Models. *CoRR* abs/2304.10592 (2023). <https://doi.org/10.48550/arXiv.2304.10592> arXiv:2304.10592

Appendix

A Victim Model Details

The details of victim large vision-language models are illustrated in Table 5. Various LVLMs employ LLMs with large number of parameters, including LLaMA [39], MPT [38], OPT [45], and Vicuna [8]. To reduce randomness, we consistently employ greedy search to generate answers for clean images or adversarial images.

Table 5: The image encoders and base LLMs of victim models.

Victim Model	Image Encoder	Base LLM
LLaVA	OpenAI CLIP ViT-L	LLaMA-2-13b
Otter	OpenAI CLIP ViT-L	MPT-7b
LLaMA-Adapter-V2	OpenAI CLIP ViT-L	LLaMA-7b
OpenFlamingo	OpenAI CLIP ViT-L	MPT-7b
MiniGPT-4	EVA CLIP ViT-G	Vicuna-7b
BLIP-2	EVA CLIP ViT-G	OPT-2.7b
InstructBLIP	EVA CLIP ViT-G	Vicuna-7b
mPLUG-Owl-2	ViT-L (non-pretrained)	LLaMA-2-7b

B Additional Experimental Results

B.1 Attack Results on Latest LVLMs

We conduct experiments on some newly released models and the results are shown in Table 6. The results indicate that our method is applicable to newly proposed LVLMs.

Table 6: Additional attack results against latest LVLMs.

Model	Clean	E2E	CLIP-Based	VT-Attack
InternLM				
XComposer2-7B [15]	32.17	26.11	-	20.43
Honeybee-7B [14]	32.57	25.49	23.23	19.94

B.2 VT-Attack Results against Different LVLMs

We provide additional qualitative results of VT-Attack against different LVLMs. Table 8, Table 9 and Table 10 present the results of attacking LLaVA [26], MiniGPT-4 [48] and mPLUG-Owl2 [42]. It can be observed that our proposed VT-Attack leads to outputs that are less relevant to the original answers compared to the baseline methods. This further illustrates the greater disruption caused by VT-Attack on information in visual tokens.

B.3 Results of Same Adversarial Image Attacking Various LVLMs

Figure 9 and Figure 10 present the additional comparison of the answers generated by different LVLMs when taking the same clean image and adversarial image as inputs. It can be observed that the same adversarial image leads to different outputs from different models. This indicates that the adversarial images whose encoded visual tokens are disrupted may not exhibit strong semantics; otherwise, different models should generate similar outputs.

B.4 Breakdown of LLaVA to Non-Visual Question Answering

In experiments we have observed that when adversarial images generated by VT-Attack are input to LLaVA [26], the question-answering capability of LLaVA not only exhibit failure to image-based queries, but also break in addressing non-visual prompts. Even when the questions posed are unrelated to the images such as "What is artificial intelligence?", the model fails to provide reasonable responses. An example is depicted in Table 11. One possible reason is that the intermediate module of LLaVA is only a linear layer with a significantly smaller number of parameters. Therefore, LLaVA is more sensitive to corrupted visual tokens compared to other LVLMs, even when queried with non-visual questions.

C Attack Performance over Iterations

The influence of attack iterations on attack performance (CLIP score) is illustrated in Figure 11, taking LLaVA [26] as an example. Increasing the number of attack iterations generally enhances the attack effectiveness. However, the improvement becomes less significant when the number of iterations exceeds 800.

D Prompts for Different Tasks

To investigate the generality of adversarial examples across different prompts, we employ three question-answering tasks. Below are prompts used for image captioning task.

1. Describe this image briefly in one sentence.
2. Give a brief description of the image.
3. Can you provide a brief description of this image?
4. Offer a brief caption for this image.
5. Give a short overview of this image.
6. Provide a short summary of this picture.
7. Describe this picture in a few words.
8. Summarize this image briefly.
9. Please provide a short title for this image.
10. Briefly explain what is shown in this image.

The prompts for general VQA are illustrated below.

1. Is there a mobile phone in this image?
2. Is there any text or writing visible in the image?
3. Can you see any shoes in this image?
4. How many pens are visible in this picture?
5. Any signs of human activity in the image?
6. Where was this image taken?
7. Can you see animals in this image?
8. Can you identify any vehicles?
9. Are there any objects related to food?
10. Do you notice any body of water?

The prompts for detailed VQA are shown as below.

1. Can you provide a detailed description of this image?
2. Can you describe the overall composition of the image?
3. What are the specific details depicted in this picture?
4. Explain the background elements in the picture.
5. Offer a comprehensive representation of this picture.
6. Give a detailed account of this image.
7. Offer a detailed analysis about the content of this image.
8. Can you describe the objects or scenery in the picture?
9. Elaborate on the elements captured in this photograph.
10. Provide a thorough description of this image.

E Sensitivity to Pixel Noise Defense

Adding tiny Gaussian noise to adversarial images is a simple way of model defense. To investigate the sensitivity of adversarial examples to it, we conduct experiments for BLIP-2 [24] as an example, and the results are shown in Table 7. Adversarial images are not sensitive to pixel noise if the size is relatively small. When the noise size exceeds 5/255, the attack performance starts to decline. However, overall,

Gaussian noise within the same magnitude (8/255) as adversarial perturbations does not significantly affect the attack performance.

Table 7: The impact of adding Gaussian noise to adversarial images on attack performance (CLIP Score ↓) compared to clean images.

Noise Size	Clean	Adversarial
0/255	30.44	20.32
1/255	30.41	20.41
2/255	30.47	20.37
3/255	30.19	20.36
4/255	30.38	20.48
5/255	30.55	20.77
6/255	30.21	21.12
7/255	30.37	21.90
8/255	30.29	22.67

Table 8: Additional cases of attack results against LLaVA [26] in different methods.

Image	Method	LVLm-Output	Image	Method	LVLm-Output
	No Attack	a group of monkeys on a tree		No Attack	a row of police cars parked on a city street
	E2E [34]	a tree filled with many birds		E2E [34]	two green police cars driving down a street
	CLIP-Based [9]	a black bear holding an object		CLIP-Based [9]	a clock on a building, a truck, and a person
	VT-Attack	a person holding a cup		VT-Attack	a white building with a clock
	No Attack	a white dog sitting on the grass		No Attack	a plaque on a brick wall
	E2E [34]	a large dog walking through the snow		E2E [34]	a close-up of a gravestone with a name on it
	CLIP-Based [9]	a dog with a collar and a tag		CLIP-Based [9]	a building with a sign on it
	VT-Attack	the a question, the the, the, the		VT-Attack	a a, a, a, a a, a a, a a a in the
	No Attack	a young boy standing next to a fire truck		No Attack	a hummingbird perched on a thin branch
	E2E [34]	an elderly woman walking down the street		E2E [34]	a bird standing on a bamboo stick
	CLIP-Based [9]	two women posing for a picture in a park		CLIP-Based [9]	a bird with a long beak on a wooden pole
	VT-Attack	a man is holding a red cell phone		VT-Attack	the question, the question, the, the question
	No Attack	a pile of yarn sitting on a table		No Attack	a small brown and white dog lying on the grass
	E2E [34]	a crochet hook and a ball of yarn		E2E [34]	a large brown dog playing with toy horses
	CLIP-Based [9]	a pair of old, worn-out leather boots		CLIP-Based [9]	a large brown bear with paws
	VT-Attack	a yellow cloth bag with a yellow cloth		VT-Attack	a person is seen holding a piece of wood
	No Attack	a bottle of Fanta and a can of Coca-Cola		No Attack	a pair of Nike sneakers sitting in a box
	E2E [34]	a bottle of green sauce or dressing		E2E [34]	a woman holding a large pile of shoes
	CLIP-Based [9]	a person holding a box of tissues		CLIP-Based [9]	a pair of shoes with a shredded shoe lace
	VT-Attack	a person is sitting at a table		VT-Attack	the the, the, the, the, the, the, the

Table 9: Additional cases of attack results against MiniGPT-4 [48] in different methods.

Image	Method	LVLm-Output	Image	Method	LVLm-Output
	No Attack	a man and a woman in a sailboat		No Attack	a carriage being pulled by horses
	E2E [34]	two people are sitting on a sailboat		E2E [34]	a carriage is being pulled by a man
	CLIP-Based [9]	a group of people on a boat in the river		CLIP-Based [9]	a man in a suit carrying a baby in a stroller
	VT-Attack	a dog sitting on a bench		VT-Attack	a small dog pulling a toy cart
	No Attack	a large ship with waves crashing		No Attack	a group of men playing basketball
	E2E [34]	a large cruise ship sailing on the ocean		E2E [34]	two men in basketball uniforms
	CLIP-Based [9]	a book cover with a picture of a boat		CLIP-Based [9]	a group of people playing basketball game
	VT-Attack	a close-up view of a compass with a needle		VT-Attack	a man standing in front of a vintage jukebox
	No Attack	a set of two padlocks with keys		No Attack	a white box with two green lights on top
	E2E [34]	a lock on a wooden table		E2E [34]	a pile of old electronics
	CLIP-Based [9]	a set of four metal bells		CLIP-Based [9]	a plastic box with a clear plastic
	VT-Attack	a vintage jukebox with many records		VT-Attack	2003 Toyota Matrix in 3D red
	No Attack	a bird with a long, curved beak		No Attack	a man holding a bicycle on his head
	E2E [34]	two birds standing on a dirt road		E2E [34]	a young boy holding a bicycle at sunset
	CLIP-Based [9]	a group of birds sitting on the ground		CLIP-Based [9]	a person carrying a bicycle on their back
	VT-Attack	a vintage music box with a colorful design		VT-Attack	a person riding a bicycle on a path
	No Attack	a hot pot of food on a stove		No Attack	a brown bear standing on a rocky cliff
	E2E [34]	a large pot filled with food		E2E [34]	a brown bear carrying a stuffed animal
	CLIP-Based [9]	a bowl of mixed seafood		CLIP-Based [9]	a close-up view of a large clamshell on a beach
	VT-Attack	a plate of crawfish etouffee		VT-Attack	a dog with a carrot in its mouth

Table 10: Additional cases of attack results against mPLUG-Owl-2 [42] in different methods.

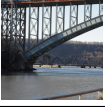
Image	Method	LVLm-Output	Image	Method	LVLm-Output
	No Attack	a man with dreadlocks plays a trumpet		No Attack	a bird sitting on a branch in the sky
	E2E [34]	a girl is playing a trumpet		E2E [34]	a man holding a baby bird in his hand
	VT-Attack	a doll is shown in two different pictures		VT-Attack	a group of people standing together
	No Attack	a bridge over a river with trees		No Attack	a brown dog panting on a sidewalk
	E2E [34]	aerial view of San Francisco bridge		E2E [34]	an ostrich wearing a hat
	VT-Attack	a close up of a pair of pants		VT-Attack	a picture of a bridge with a blue sky
	No Attack	a white and gray dog standing on grass		No Attack	a sewer cover with a metal design on it
	E2E [34]	a baby is sitting on top of a lion		E2E [34]	a castle is shown on a tire
	VT-Attack	a group of people are standing in a room		VT-Attack	two microphones are set up in a studio
	No Attack	a large building with a curved roof		No Attack	a bridge over a river with a train on it
	E2E [34]	a cruise ship in the ocean		E2E [34]	a man driving a car under a bridge
	VT-Attack	a pair of shoes with the number 43 on them		VT-Attack	a group of 777 nail polish bottles
	No Attack	a tank with people on top of it		No Attack	a baby wearing a green knitted hat
	E2E [34]	a dog driving a tank with a missile		E2E [34]	a man with a bubble on his face
	VT-Attack	a photo of a person in a black dress		VT-Attack	a close-up of a gold and black watch

Table 11: Breakdown of LLaVA to non-visual prompts when queried with adversarial image in VT-Attack.

Adversarial image	Non-visual Prompt	LLaVA-Output
	What is artificial intelligence?	in the a, a in the a, a in the a in the a in
	What is the capital of France?	a person is holding a red glass ball
	How do you bake a cake?	,,,,, in the a,,,,, in the a, a in the a in
	Why do leaves change color in the fall?	the question, the question, the question

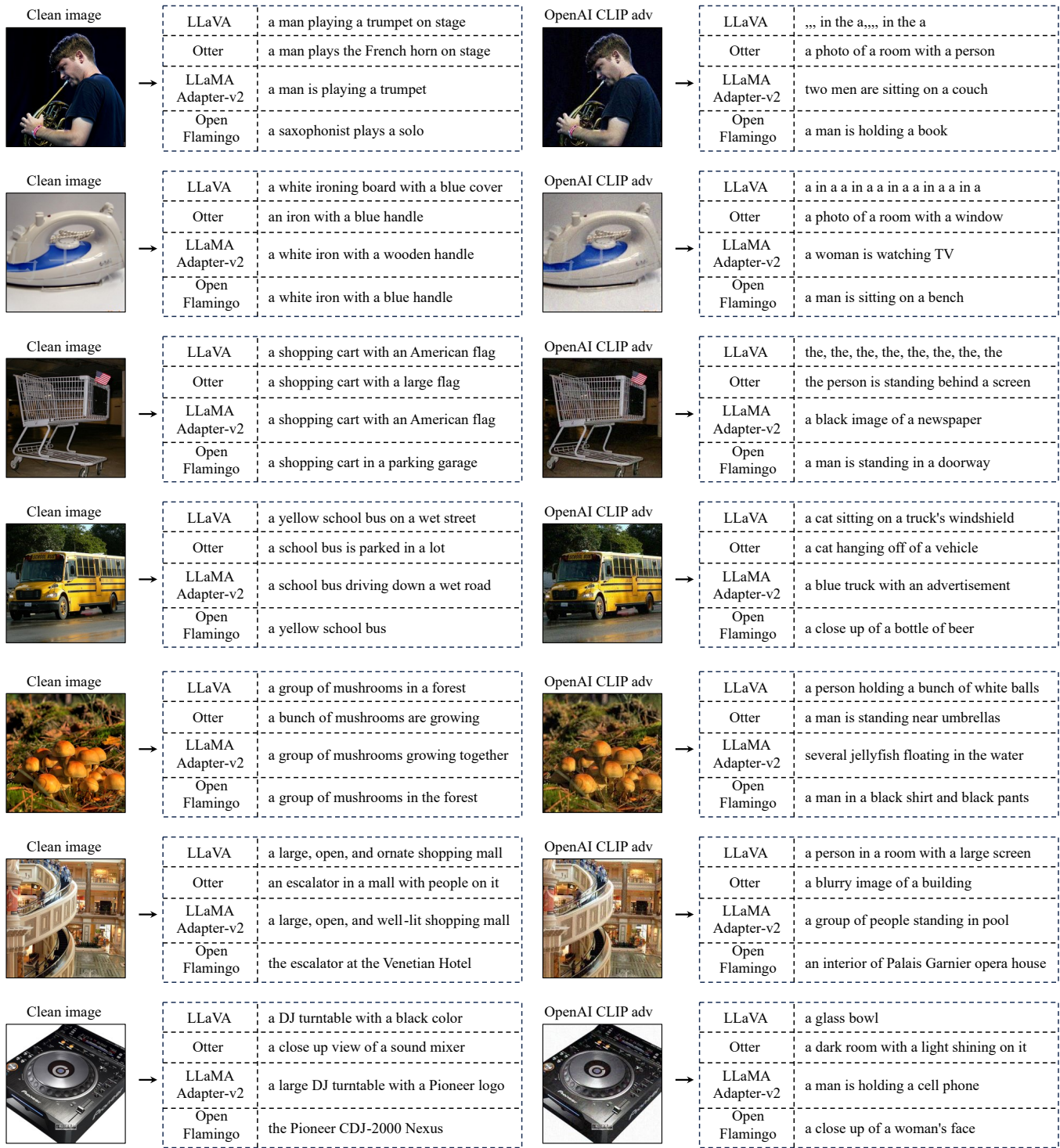


Figure 9: Additional comparison of the responses generated by various LVLMS when queried with clean images and adversarial images in VT-Attack against OpenAI CLIP [32].

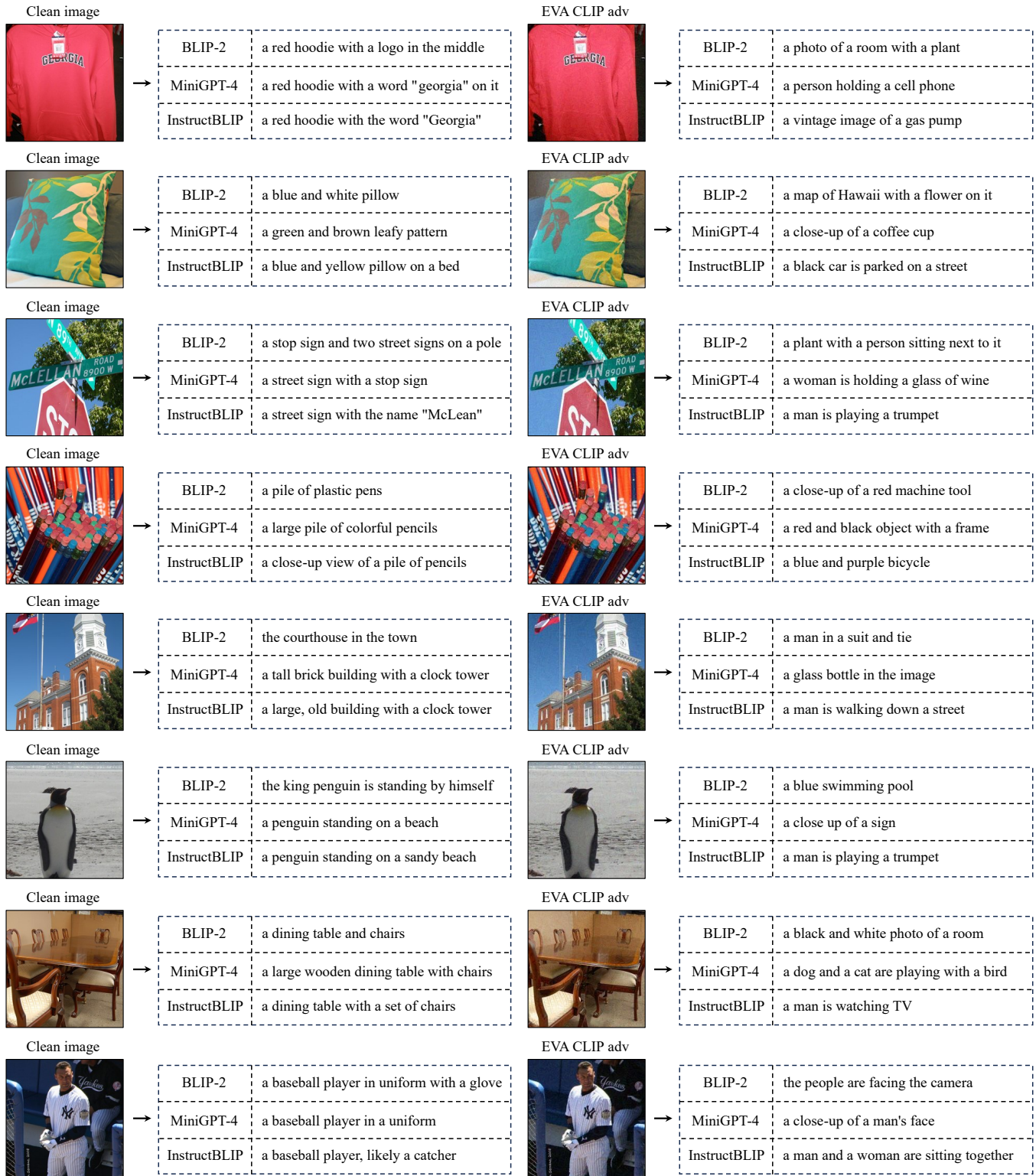


Figure 10: Additional comparison of the responses generated by various LVLMs when queried with clean images and adversarial images in VT-Attack against EVA CLIP [16].

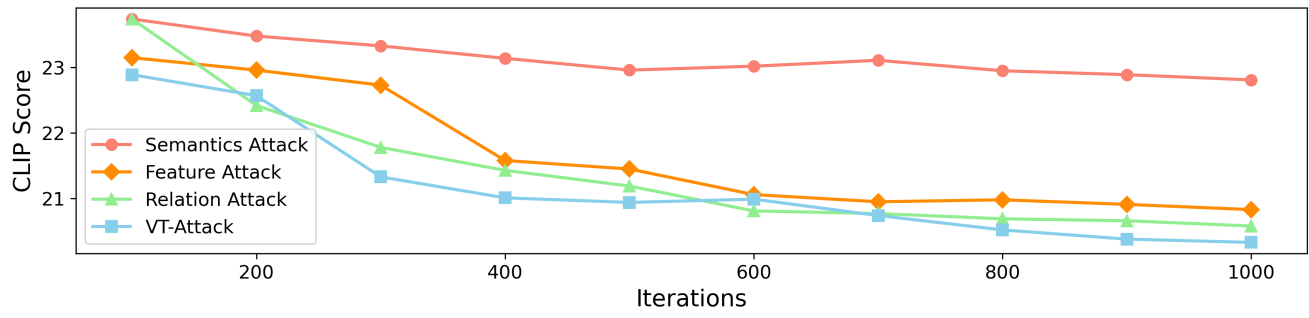


Figure 11: The relationship between attack performance and iterations (taking LLaVA [26] as an example).